A Feasibility Study of Additively Manufactured Heat Guides for Enhanced Heat Transfer in Electrical Machines

Rafal Wrobel
School of Engineering, Newcastle University
Newcastle upon Tyne, UK
rafal.wrobel@newcastle.ac.uk

Ahmed Hussein
HiETA Technologies Ltd.
Bristol, UK
ahmedhussein@hieta.biz

***Abstract*—This paper investigates a new heat extraction approach for application to high-specific-output electrical machines. The proposed technique employs thermally conductive heat guides (HGs) to provide supplementary heat evacuation paths for the machine regions, which are particularly susceptible to high power loss. Here, the research focus has been placed on the stator-winding assembly. The HGs investigated in this work rely solely on conductive heat transfer, in contrast to the solutions involving working fluid phase change, e.g. heat pipes (HPs). It is intended for the HGs to be an integral part of the stator-winding assembly, e.g. HGs incorporated in the winding active and/or end region. Such arrangement however, imposes several design challenges. These are related with the HGs being a source of additional power loss due to the machine's magnetic flux leakage. The objective of this study is to evaluate a concept of HGs, which are immune to the external magnetic field with good heat transfer capability. To facilitate that, a combination of detailed multi-physics design-optimization together with modern additive manufacturing (AM), (i.e. selective laser melting (SLM) method), has been employed here. The theoretical analysis has been supplemented with an experimental work. A number of stator-winding hardware exemplars (motorettes) incorporating alternative HGs designs have been fabricated and tested. This paper provides a new set of experimental data in support of the authors' initial work on HGs' thermal behaviour. The new research findings show that the optimised HGs allow for up to 85% improvement in dissipative heat transfer from the winding body and insignificant additional power loss, for the analysed stator-winding assembly.**

Keywords— heat guides, heat transfer, power loss, stator-winding assembly, electrical machines, additive manufacturing

I. INTRODUCTION

When designing a new high-specific-output electrical machine, the balance between the generated power loss and dissipative heat transfer needs to be carefully considered. The effective thermal management is one of the key enabling factors [1]-[10]. Examples of evacuating heat from electrical machines include the passive and active methods [4]. In both cases, the generated heat is commonly extracted through the machine's external periphery. In specific applications, the generated heat is extracted directly from the heat sources by contact with a coolant, i.e. direct gas or liquid heat evacuation [4]. The latter approach usually involves a more complicated machine design, which incorporates functionality of the thermal management system. On the other hand, the simpler heat extraction from the machine's housing requires some form of heat guiding to enhance heat transfer from across multiple materials and subassemblies. For example, the stator-winding assemblies are commonly impregnated using 'high' thermal conductivity materials (e.g. $(1-3)\,W/m\cdot℃$) or some other design features are introduced to improve the dissipative heat transfer [1]-[15]. However, such commonly-used techniques are frequently limited by various factors like the physical properties of impregnating materials, fabrication methods, or cost associated with practical implementation for in-volume manufacture among others.

In this feasibility study, a new heat extraction method, for application to electrical machines, is proposed. The technique employs thermally conductive heat guides (HGs) to provide supplementary heat evacuation paths to the machine regions, which are particularly prone to high power loss. The HGs can be manufactured as passive or active components. The passive guides rely solely on conductive heat transfer, whereas the active designs additionally employ materials with phase change, e.g. heat pipes (HPs). This investigation focuses on heat evacuation from the stator-winding assembly, which is usually the main heat source in electrical machines. Only passive HGs are analysed in this study. It is important to note that the use of active components like HPs, to improve heat management in electrical machines, has been reported in the literature [1], [3]. Also, some other forms of heat guiding have been investigated by other authors [4], [10]-[15]. However, practical implementation of any of the HG solutions requires careful consideration.

The proposed HGs, are intended here to be an integral part of the stator-winding assembly and are mounted in close proximity to the winding, for example, HGs placed within the stator slots to enhance heat transfer from the winding's active length and/or HGs located by the winding's ends to improve heat extraction from the machine end-regions. Clearly, any electrically conductive parts placed near the winding body will be exposed to the time and spatial variation of magnetic flux

leakage, and consequently such components will generate additional power loss. Therefore, the use of solid metallic HGs would provide negligible improvement, if any, to the overall system performance, particularly when considering high-speed/high-frequency machine designs. It is important to note here that the thermal and electrical conductivities of metallic materials are closely related, and a 'good' thermal conductor (e.g. copper $398\,W/m\cdot℃$ and aluminium $210\,W/m\cdot℃$) also has 'good' electrical properties (e.g. copper $1/1.72e-8\Omega m$ and aluminium $1/2.82e-8\Omega m$). This imposes clear design challenges for HGs, where the enhanced heat transfer and additional power loss need to be well balanced.

The initial results have shown that a combination of detailed multi-physic design-optimisation and modern additive manufacturing enables HG solutions with minimal additional power loss. Here, selective laser melting (SLM), a laser-driven metal powder-bed version of additive manufacturing has been used. The use of SLM allows fabrication of complex and optimised heat sink features that otherwise would be difficult to make using conventional manufacturing techniques. A HG, which is immune to the external magnetic field with good heat transfer capability would be very desirable. The main objective of this work is to assess feasibility of such HG concept, in the context of the next generation of high-specific-output electrical machines. This paper expands the authors' earlier research, which was focused mainly on power loss generated in the HGs with some elements of thermal analysis [15]. Here, the theoretical body of work devoted to thermal behaviour of HGs has been supplemented with experiments on a set of hardware exemplars. Both, the experimental approach used in thermal characterisation of HGs and measured results are discussed in detail, in this expanded paper. The results show that the optimised HGs allow for up to 85% improvement in dissipative heat transfer from the winding body and insignificant additional power loss, for the analysed stator-winding assembly. The improved heat removal directly translates to increased winding power loss handling of approximately 40% and 20% at the low and high ends of the operating frequency range, respectively.

II. Hardware Exemplars

Fig. 1a) presents an outline of the stator-winding assembly incorporating HGs, which are placed in the stator slots for extracting heat from the winding's active length. The stator-winding is representative of a permanent magnet (PM) machine (rated power, 80kW and rated rotational speed, 7,500rpm). The stator is laminated using electrical steel (M250-35A), and the double-layer precision-wound concentrated winding uses copper round-profile conductors with class H (180°C) enamel coating. A slot liner material (PEEK) is used to provide an electrical separation between the stator core pack and conductors, and HGs and conductors. The complete stator-winding assembly is encapsulated using high thermal conductivity epoxy resin (Epoxylite EIP4260) to assure a good heat transfer from the stator-winding assembly to the machine housing, which is actively cooled. The coolant inlet temperature is controlled and set to 60°C.

A reduced stator-winding assembly sector (motorette) with a single coil and the neighbouring stator tooth-segments has been chosen for experimental work in this feasibility study. Such a setup provides an exact geometrical representation of a slot in the complete stator-winding assembly. This is essential when analysing the power loss components [7]-[9]. The motorette hardware evaluation has been selected here to reduce cost and time associated with the prototyping and testing full motors [5]-[9]. Fig. 1b) presents a motorette exemplar together with constituent components prior to final assembly and impregnation. The core pack assembly is heat shrunk into the aluminium interfacing plate to provide a good contact between the parts. The HGs shown in Fig. 1b) are made of aluminium alloy (AlSi10Mg). The individual HGs are inserted in the slots (two per slot) and then securely mounted to the interfacing plate. It is important to note that only a half of the HG width across the stator slot is required for the motorette experimentation.

a)

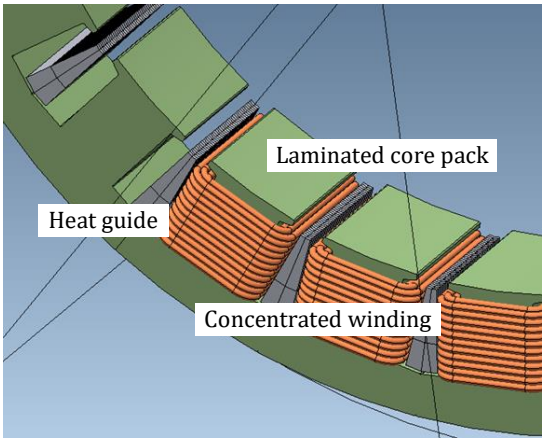

b)

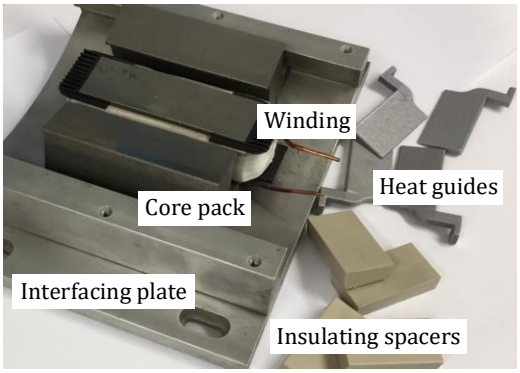

Fig. 1. Outline of the stator-winding assembly a) concept of the stator-winding with HGs placed in the stator slots – 3D FE model representation, b) motorette hardware prior to final assembly and impregnation

To emulate adiabatic boundary condition between neighbouring coils, i.e. no heat transfer across individual coils, a set of insulating blocks (PEEK) are placed in the slot cavities for the remaining coils. A single motorette is instrumented with several type-K thermocouples placed in the winding active and end regions, and stator core pack (back iron and tooth body). Such constructed hardware exemplars allow for both thermal and power loss analysis and are sufficient to inform the low additional power loss and enhanced heat transfer HG design [5]-[10]. However, the motorette hardware does not provide complete insight into the power loss generated in the winding at

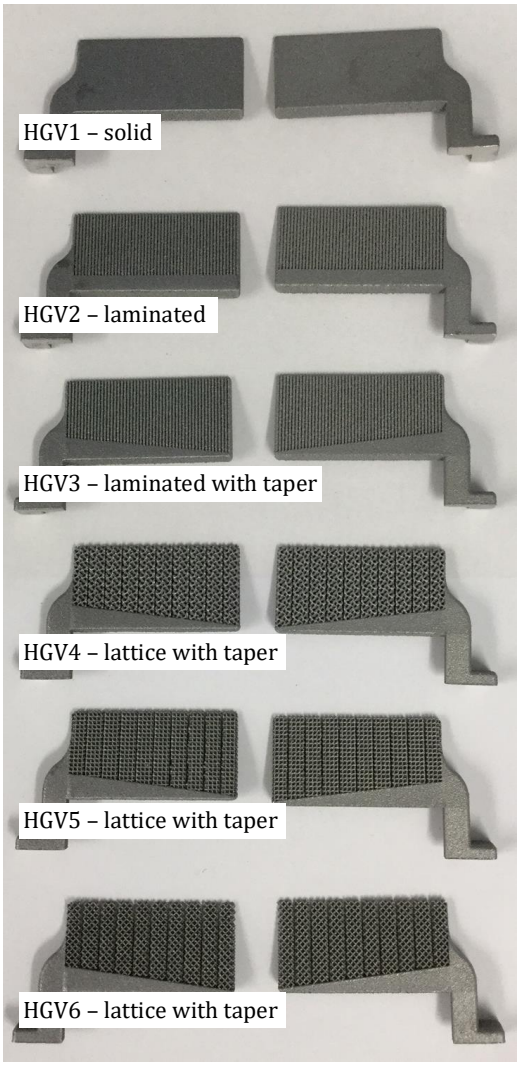

Fig. 2. Alternative HG designs

ac operation, as the contribution of neighbouring phases to the overall loss is not accounted for [7]. Also, the rotational ac effects are not considered here. These however, can be evaluated theoretically for the complete stator-winding using a finite element analysis (FEA) [7]-[9], some of which are discussed later in the paper. Fig. 2 presents six alternative HG designs considered in the study. These have been selected based on the theoretical analysis, details of which are presented in the following sections of the paper. The heat guide variants (HGVs) include solid construction (HGV1), laminated construction (HGV2-HGV3) and lattice construction (HGV4-HGV6). The motorette design without HGs in place is used here as a baseline for benchmarking both power loss and heat transfer performance measures. It is important to note that the slot utilisation for the baseline design is lower than commonly used. However, this is not unusual and is frequently attributed to the limitations of a specific winding manufacturing technique and design choices for the windings with low power loss at ac operation, and good heat transfer [8], [9].

III. Theoretical Analysis

To enable a HG design combining the good heat transfer and low additional power loss, a detailed analysis combining both electromagnetic and thermal effects is required. In this feasibility study, a three-dimensional (3D) FE approach has been employed in the design process. Clearly, the requirements for the HG design are conflicting when considering solid metallic materials. A metallic material with good thermal conductivity has usually good electrical conductivity, which will most likely lead to additional machine power loss at ac operation. Here, a design concept utilising an appropriate lamination, assuring poor equivalent electrical conductivity, but good equivalent thermal conductivity is investigated. By the use of appropriate fabrication, the equivalent electrical and thermal properties of the HG become anisotropic. The material properties for selected axes of the HG are altered to provide the good heat transfer and low power loss simultaneously. The theoretical analysis presented in this paper is limited to a more conventional method of altering physical properties to achieve material anisotropy. An axial lamination of the HG's body is discussed here in detail, with the research findings feeding into alternative HG designs fully utilising SLM additive manufacturing.

A. Power Loss Separation

A detailed power loss analysis for the laminated HG concept has been performed. Here, a portion of the HG assembly is axially laminated to reduce the ac power loss due to the slot magnetic flux leakage. The solid spine of HG assures well defined heat transfer path to the heat sink. A number of alternative design variants have been analysed, where the ratio of height of the laminated part to total HG height is altered, $k_{lam} = (h_l/(h_s + h_l))$, Fig. 3. The solid HG design represents here the worst case in terms of the additional power loss. It has been assumed that the HG is manufactured from aluminium alloy to ensure good heat transfer and low weight design. Two HGs, which are inserted into the slot from opposite ends of the stator-winding assembly, are used per slot.

All power loss components including the winding's individual conductors, stator core, and HG, for ac sinewave current excitation and fundamental frequency range up to 1kHz, are accounted for. The temperature variation of the ac power loss is also considered. The 3D FE model of the stator-winding incorporating HG is schematically shown in Fig. 1a). It is important to note that Fig. 1a) presents the model of the complete stator-winding assembly accounting for neighbouring phases and multiple HGs. The motorette analysis discussed in this section uses a simpler model definition with a single coil/phase and half-width HGs. Both HGs and the individual winding's conductors are defined as solid conductors in the FEA. The model regions representing conductors are configured using an appropriate external circuit to form required electrical connections. Here, all conductors within a single coil are connected in series, whereas the winding phases are star connected, where appropriate. The magnetic non-linearity of the core material is also accounted for. However, for the stator-winding or motorette analysis the magnetic saturation is of lesser importance as compared to the complete machine assembly, where the core pack operates at higher magnitude of the

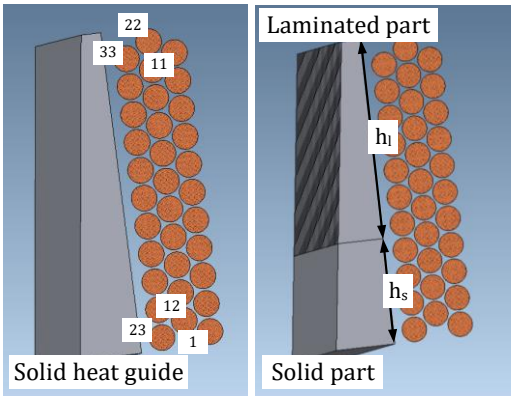

Fig. 3. Outline of the solid and partially laminated HG variants together with labels; here, the lamination thickness is fixed and equal to 1.0mm; conductor diameter is equal to 1.7mm

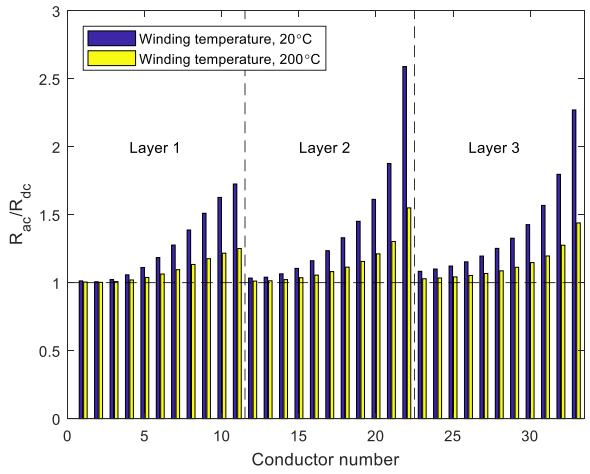

Fig. 4. Winding R_{ac}/R_{dc} at reference sinewave current excitation, 1kHz fundamental frequency (f) for motorette without HG assembly; here, the excitation current is equivalent to $4.5A_{rms}/mm^2$ per conductor dc

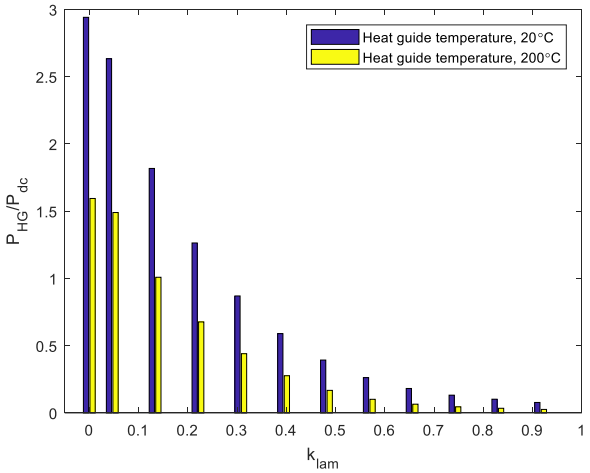

Fig. 5. Ratio of the additional HG power loss at ac operation to the dc winding power loss at reference excitation sinewave current, $f = 1$kHz

magnetic flux density. As expected, the change of magnetic flux leakage is the most severe in the slot opening region. Consequently, the ac power loss contribution of the stator-winding assembly parts exposed to this portion of the magnetic flux leakage is the highest [8], [9]. Fig. 4 shows per conductor increase of the dc winding resistance at ac operation derived as $(R_{ac}/R_{dc})|_{I,T=const} = (P_{ac}/P_{dc})|_{I,T=const}$ to illustrate that effect, where the conductor numbering indicate consecutive coil layers, i.e. layer 1: 1 to 11, layer 2: 12 to 22 and layer 3: 23 to 33. A similar trend can be observed when analysing the ac power loss associated with the HG assembly, Fig. 5. Here, the HG power loss is normalised to the winding dc power loss showing that the additional power loss is prohibitively large for the HG variants with large portion of solid assembly. $k_{lam} = 0$ represents solid HG design, whereas $k_{lam} = 1$ indicates fully laminated alternative. Also, a strong impact of the HG temperature on the generated power loss is observed, with approximately 50% loss reduction when comparing calculated data for 20°C and 200°C. The close relationship between the ac winding and HG power loss provides clear design directions for a low power loss HG solution.

To accelerate thermal assessment of the HG design variants, a functional representation for the individual power loss components as a function of dc winding power loss has been derived. For example, the HG power loss as a function of dc winding power loss, excitation frequency and winding temperature can be written in the following form,

$$P_{HG}|_T = I_{dc}^2 R_{dc}|_{T_0} \frac{\left(\frac{P_{HG}}{P_{dc}}\right)\Big|_{T_0}}{\left(1+\alpha(T-T_0)\right)^{\beta}} \qquad (1)$$

where, $I_{dc}^2 R_{dc}|_{T_0}$ is the winding dc power loss at reference temperature T_0 (here, $T_0 = 20$°C), P_{HG} is the HG power loss generated at ac operation, α is the temperature coefficient of electrical resistivity for the HG material (here, $\alpha = 4.3 \times 10^{-3}\ 1/$°C) and β is derived from curve fit to the P_{HG} data at two temperatures, e.g. T_0 and maximum intended operating temperature.

The ratio $(P_{HG}/P_{dc})|_{T_0}$ needs to be derived just once for a set of frequencies, temperature T_0 and given reference P_{dc}, allowing then for the HG power loss to be derived at any input current. Similar functional representations were derived for both winding and core power loss components [7]-[10]. These, however, are not included here due to conciseness of the paper. A complete set of the formulae allows to significantly speed up thermal analysis, where the generated power loss needs to be iteratively updated with temperature. This is particularly important for the winding and HG regions. Also, such form of expressing the individual power loss components allows for deriving operating thermal envelope of a complete machine or motorette as function of the excitation parameters, i.e. excitation current magnitude and frequency.

B. Heat Transfer Assessment

To evaluate thermal behaviour of the individual HG design variants, a number of supplementary thermal 3D FEAs have been performed. It is important to note that the intended heat transfer mechanism within the stator-winding assembly is due to conduction. The generated heat is conducted and dissipated in

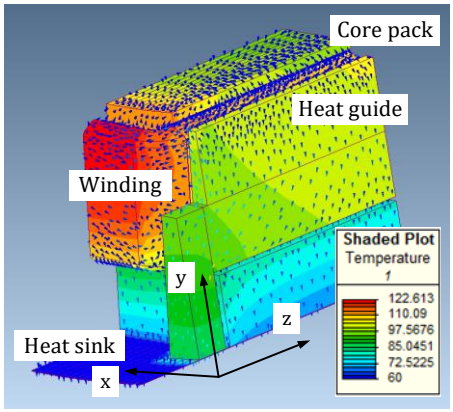

Fig. 6. An example temperature distribution and heat flux distribution for dc winding excitation; here, HG with $k_{lam} = 0.57$ and interfacing feature is shown; (temperature distribution in °C)

the liquid cooled, temperature-controlled housing, which is emulated by an appropriate cold plate for the motorette analysis. Also, the heat transfer mechanisms within the complete stator-winding and motorette assemblies are equivalent. Fig. 6 presents thermal model representation of the stator-winding together with heat flux distribution. The encapsulating epoxy resin is not shown here. The winding is excited with dc current that is representative of dc thermal testing [5], [6]. For such operating condition, only dc winding power loss component is present, allowing for the winding-to-stator heat transfer to be accurately derived. A quarter of the stator tooth with a single coil is sufficient here to evaluate the thermal behaviour. It has been assumed that outer surface of the stator back iron is the only path for the generated heat to be evacuated. Here, a fixed temperature boundary condition of 60°C is set. The remaining surfaces of the model are adiabatically insulated. This represents the worst-case scenario for a machine operation, where the other heat transfer mechanisms are not present, i.e. no heat transfer across the air-gap nor from the end-winding region due to convection or radiation. The contact thermal resistances have been initially assumed based on the authors' previous experience and available literature, by appropriately adjusting equivalent thermal conductivity for the contact regions, i.e. winding-to-stator or stator-to-housing interfacing layer. Here, the equivalent contact airgaps are equal to 10μm and 2.5μm for the winding-to-stator (slot liner) and stator-to-housing regions (thermal paste) [5], [19].

TABLE I. THERMAL MATERIAL DATA FOR IMPREGNATED MOTORETTE ASSEMBLY

Model region	$[W/m \cdot ℃]$	$[J/kg \cdot ℃]$
Winding[1)]	$k_x = k_y = 3.5, k_z = 229.3$	474
Core pack	$k_x = k_y = 22.2, k_z = 4.9$	304
HG (solid)	$k_x = k_y = k_z = 230.0$	900
HG (laminated)	$k_x = k_y = 222.2, k_z = 36.4$	908
Epoxy resin	$k_x = k_y = k_z = 0.85$	1700
Slot liner[2)]	$k_x = k_y = k_z = 0.25$	1260
Thermal paste[3)]	$k_x = k_y = k_z = 0.25$	1260

[1)] thermal properties for the winding active length; [2)] $0.34\ W/m \cdot ℃$ and [3)] $2.9\ W/m \cdot ℃$ before adjusting for the contact air-gaps

Table I includes complete list of thermal material data used in the analysis. The equivalent thermal conductivity for the impregnated winding, HGs and laminated core pack accounts for the regions' anisotropy. Data for the winding and laminated

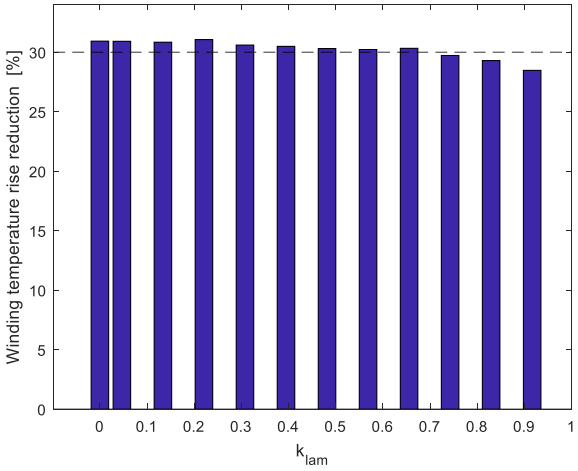

Fig. 7. Percentage reduction of the winding temperature rise for alternative HGs designs

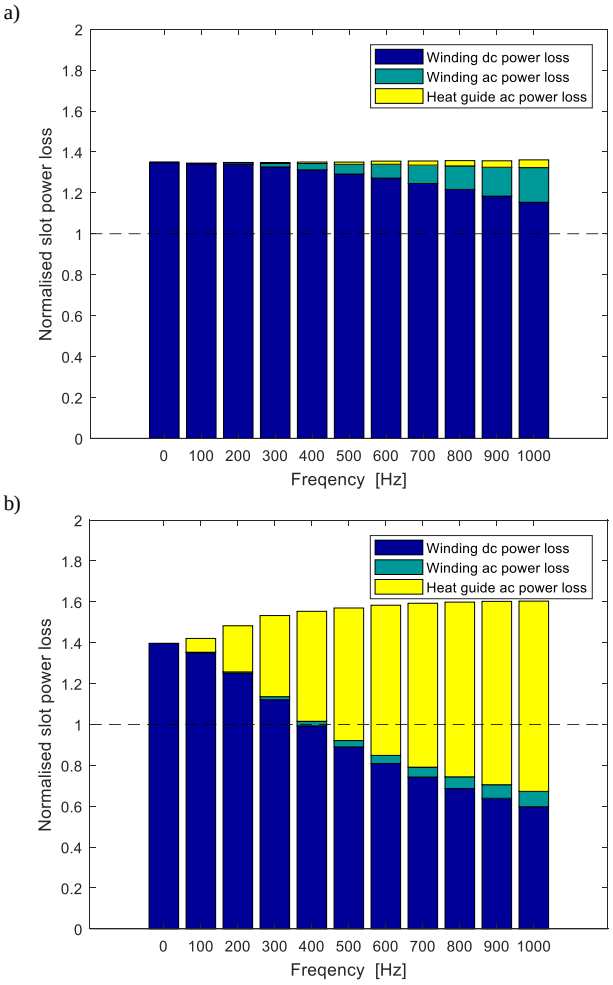

Fig. 8. Normalised power loss envelope for 180°C winding hot-spot temperature versus excitation frequency, a) $k_{lam} = 0.91$ – well laminated HG body, b) $k_{lam} = 0$ – solid HG body

core pack has been informed from tests on appropriate material samples [17]. Fig. 7 presents percentage reduction in the winding temperature rise for the analysed HG designs with the lamination variant equivalent to that for HGV2. The results show approximately 30% improvement as compared with the baseline design without HGs. There is a small variation among the design variants. This results from poorer axial heat transfer for HGs with reduced cross-section of the solid spine, i.e. k_{lam} is large. Interestingly, when analysing the results two thirds of the overall improvement in heat transfer is associated with the heat path in the plane of the stator-winding assembly, (xy plane in Fig. 6). The remaining one third is due to heattransfer along active length of the winding, (z axis in Fig. 6) into the heat sink. This balance might differ depending on stator-winding and HG design. For example, if the HG solid spine was replaced with a HP alternative.

The initial thermal evaluation with dc winding excitation is insufficient to draw complete conclusions regarding optimal HG design. Consequently, a more in-depth thermal analysis combining all ac power loss components has been carried out. Fig. 8 presents calculated winding and HG power losses as a function of excitation frequency. All power losses in Fig. 8 have been derived assuming 180℃ winding hotspot temperature limit. The overall allowable power loss and its distribution has been calculated by iteratively adjusting dc winding power loss of the power loss functions discussed earlier, e.g. (1). Here, the theoretical predictions have been normalised to the baseline motorette design at dc operation. The presented results represent two extremities of the analysed HG variants, $k_{lam} = 0.91$ for well laminated HG body (almost entire HG height is laminated) and $k_{lam} = 0$ for solid HG body (no laminated part is present). It is evident that at lower excitation frequencies the HGs perform in a similar manner with approximately 40% increase in dc winding power loss handling. This directly translates to higher input current magnitude by 20%. The calculated data for higher frequencies revealed that HGs are also capable of enhancing current handling for that operating region, here approximately by 10%, Fig. 8a). Clearly, all these would have a significant impact on power output capability of a machine equipped with HGs. It is worth remembering here that the above analysis is for the lamination variant HGV2.

The authors' previous work provides more insight into the ac power loss effects for all analysed HG variants [15]. The calculated results suggest that HGs with k_{lam} from 1.0 to 0.5 seem to provide the best overall performance gains. Further to these, the results show that the overall power loss, which it is possible to dissipate from the motorette assembly is the highest for solid-like HG designs, i.e. $k_{lam} \approx 0$, Fig. 8b). Here, approximately 60% increase in the power loss handling has been found. This might be counterintuitive, but the power loss generated by the HGs is relatively easy to dissipate as compared with the winding region, Fig. 8b). Another interesting effect is related to the winding ac loss component, which is reduced for solid-like HGs. The HG shielding effect observed here is similar to that discussed for inductor design [18].

IV. Experimental Validation

A. Power Loss Analysis

One of the key factors when comparing multiple hardware exemplars is the repeatability of manufacture, which might affect the overall research findings. To make sure that any measured differences among the motorettes is due to alternative HG designs, all motorettes without HGs in place were tested using the experimental setup shown in Fig. 9. The setup allows for measuring ac loss contribution in the motorette assembly by analysing frequency variation of impedance [23]. Fig. 10 shows such variation of the measured and calculated increase of the winding dc resistance at ac operation (R_{ac}/R_{dc}) for all motorettes. The results show good correlation between the measured and calculated data.

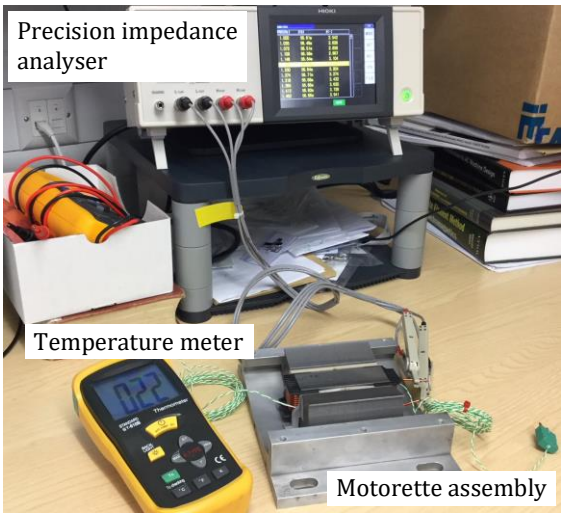

Fig. 9. Experimental setup for deriving ac loss contribution

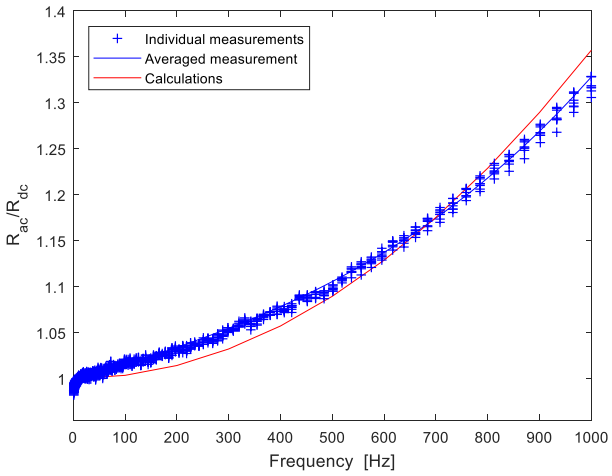

Fig. 10. Increase of winding dc resistance at ac operation versus excitation frequency at room temperature ($T = 20$℃)

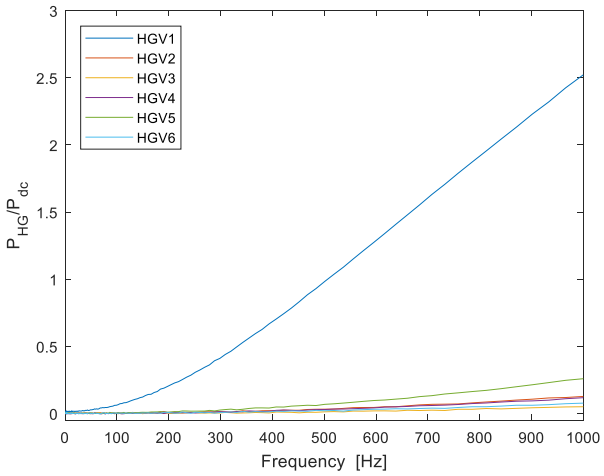

Fig. 11. Measured HG power loss contribution as a ratio of winding dc power loss versus excitation frequency at room temperature ($T = 20℃$)

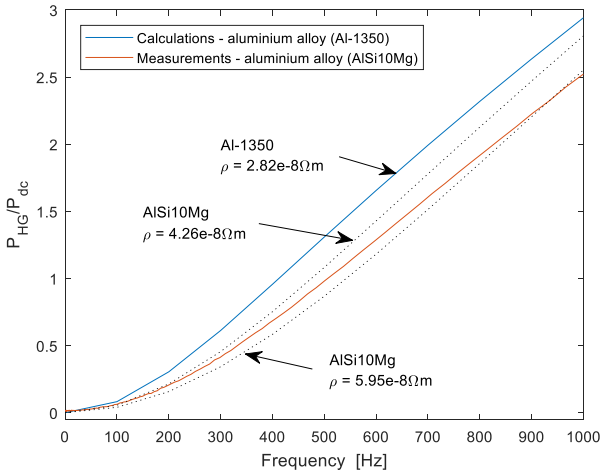

Fig. 12. Frequency variation of HG power loss contribution in reference to the winding ac power loss (P_{HG}/P_{dc}) at room temperature ($T = 20℃$)

Also, the measurement spread is relatively low. All these provide a good base for the motorette tests with HGs. It is important to note that the winding ac power loss contribution presented in Fig. 10 was separated from the core power loss using an experimental superposition. A motorette assembly with a low ac power loss winding was used to divide the power loss components [24].

Fig. 11 presents measured data from tests on the motorettes with alternative HG variants. Here, frequency variation of the HG power loss contribution, normalised to dc winding power, loss (P_{HG}/P_{dc}), is provided. The HG power loss contribution was separated from other power loss components assuming that R_{ac}/R_{dc} is identical for all analysed motorettes, i.e. shielding effect of the alternative HGs is not accounted for. As expected, the laminated HG variants, HGV2-HGV3 assure low additional power loss to the overall stator-winding power loss balance. Also, HGs with alternative lattice structures perform well, HGV4-HGV6. Here, HGV6 assures the lowest additional power loss contribution among the analysed design variants, 76 times reduction of P_{HG}/P_{dc} as compared with solid HG (HGV1). It is worth remembering that the presented results have been measured at room temperature, 20℃ . At elevated temperatures the ac effects induced in HGs are expected to be considerably reduced, due to change in electrical resistivity with temperature of the HG's material, e.g. Fig. 5.

Fig. 12 compares measured and calculated results of P_{HG}/P_{dc} for HGV1. When analysing the results there is a clear discrepancy between both results.

a)

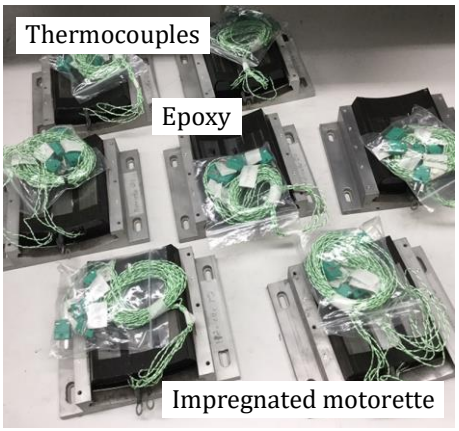

b)

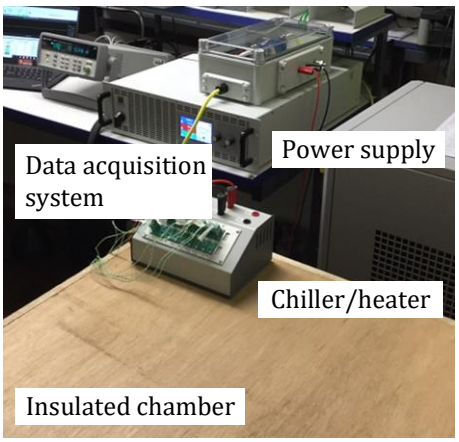

c)

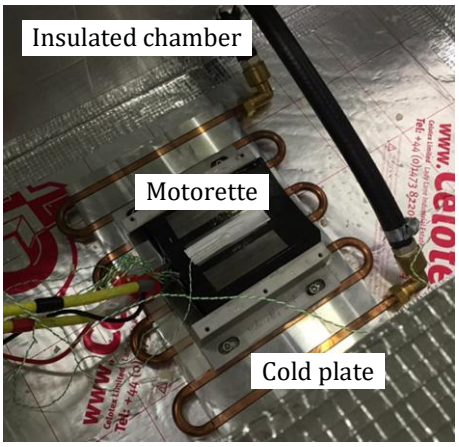

Fig. 13. Experimental setup for characterising thermal performance of HGs, a) complete set of impregnated and instrumented motorettes, b) test rig with individual components, c) single motorette mounted on a temperature controlled cold plate, inside the insulated chamber

Initially, in the analysis, it was assumed that HG material has physical properties equivalent to those for aluminium alloy (Al-1350) used for electrical conductors. However, when considering additive manufacture employing SLM technique, there is a variety of aluminium alloys that could be chosen. Here, aluminium alloy (AlSi10Mg) was used [20]-[22]. It is important to note that physical properties of parts made of AlSi10Mg depends on post fabrication treatment, e.g. annealing or heat treatment [20]. For example, the electrical resistivity of AlSi10Mg is in range from $4.28e-8\Omega m$ to $5.95e-8\Omega m$ as compared to Al-1350 $2.82e-8\Omega m$ [20]. In this study, data derived in [20] has been used to correlate the measured and calculated results. The dashed lines in Fig. 12 show P_{HG}/P_{dc} predictions calculated for extremities of the electrical resistivity range. The results indicate that the measured data is within the theoretically derived boundaries.

B. Transient Thermal Analysis

Thermal behaviour of the alternative motorettes considered in this investigation is another important design aspect. Some theoretical predictions have been presented in the authors' earlier work showing a significant improvement in extracting heat from the winding body [15]. Both transient and steady state thermal behaviours were analysed. In this extended paper, the experimental body of work from thermal tests is discussed in detail. Fig. 13 shows the hardware motorettes and experimental setup used in thermal tests. The complete family of impregnated and instrumented motorettes is shown in Fig. 13a). Here, a set of type-K thermocouples placed in the winding-end and -active regions together with tooth body, back-iron and interfacing plate was used to monitor temperature for each of the motorettes. Multiple thermocouples have been used in each specific region of the motorette assembly to provide a more reliable, averaged thermal data. The complete experimental set up includes the insulated chamber, temperature-controlled liquid-cooled cold plate, chiller/heater unit, dc power supply, current and voltage transducers, and data acquisition system. The insulated chamber emulates an adiabatic boundary condition for all the motorette surfaces, which are not in contact with the cold plate. The experimental setup allows for well-defined and repeatable testing conditions, where the generated heat is dissipated via the temperature controlled heat sink (cold plate).

Prior to thermal tests, a number of hardware checks of the experimental setup were carried out. This is to make sure that initial assumptions regarding the heat transfer paths are satisfied. Fig. 14 shows an example thermal image illustrating a good thermal separation for the central tooth with energised coil and neighbouring teeth with insulating spacers. This was also confirmed by measured thermal data gathered from the thermocouples. Fig. 15 presents an example of measured thermal transients for the baseline motorette and motorette with solid body HG (HGV1). Here, a thermal step response to approximately 80W of initial input power is shown. Both, the winding-end and -active region temperature rise transients above the cold plate temperature are presented. It is evident that HGs provide significant improvement to the overall heat transfer with approximately 30% and 40% reduction in

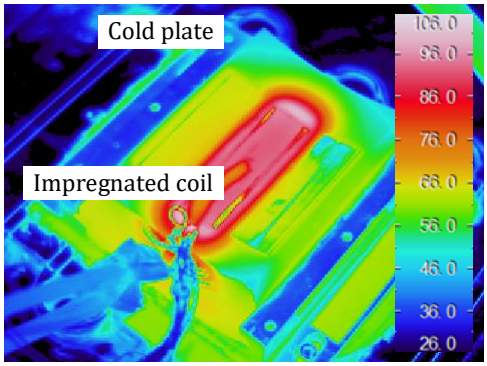

Fig. 14. An example temperature distribution in a motorette assembly – infrared image, temperature in ℃

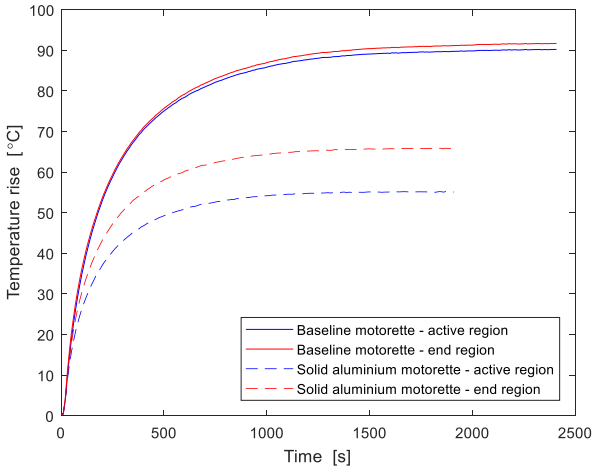

Fig. 15. Measured winding temperature rise for the baseline mottorete and motorette with solid body HG (HGV1) – thermal transients

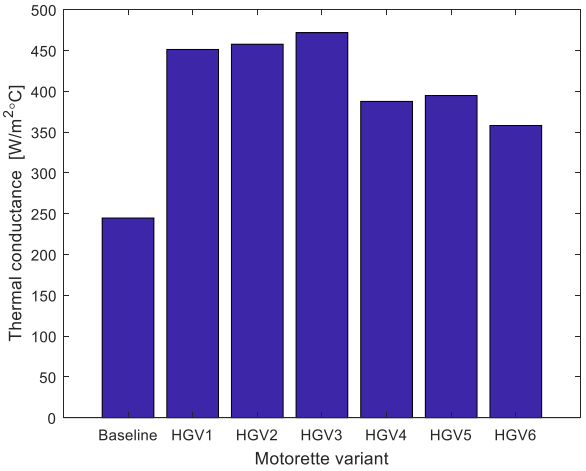

Fig. 16. Experimentally derived winding-to-stator thermal conductance

temperature rise for winding-end and -active region, respectively. When comparing results for the motorettes, it is clear that the overall improvement is due to enhanced dissipative heat transfer in the winding-active region. The characteristic difference in the temperature rise for the winding-end and -active regions (motorette with solid body HG) as compared to virtually no difference for the baseline motorette.

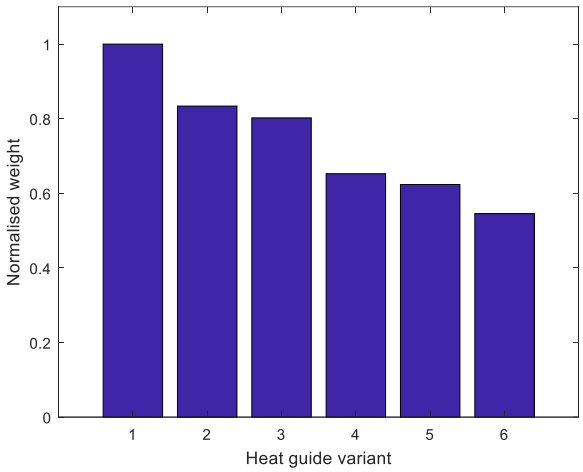

Fig. 17. Normalised weight of the alternative HG designs

The experimental findings are in line with the initial theoretical predictions discussed in the previous section of the paper, Fig. 7.

One of the generic parameters describing heat transfer from the winding body to the stator core pack/machine periphery is thermal conductance [25]. This heat transfer performance measure has been chosen here to compare all motorette/HGs variants. Fig. 16 shows the winding-to-core thermal conductance derived from thermal measurements. The results suggest significant improvement in the overall heat transfer from the winding body for all motoretts with HGs. Here, approximately 85% and 55% increase of the thermal conductance is shown for motorettes with HGV1-HGV3 and motorettes with HGV4-HGV6, respectively. When analysing the data, it is clear that the more conventional laminated HG design provides an all-round solution both in terms of low additional power loss and high heat transfer improvements.

The authors showed previously that the HGs have some impact on the thermal capacitance of the stator-winding assembly [15]. This results from different specific heat capacity of the aluminium alloy, which replaces a portion of the stator-winding epoxy impregnation, for the motoretts with HGs. It was found that HGs contribute up to 10% increase to thermal capacitance of the stator-winding assembly (10% refers here to motorette with HGV1). The exact figures depend on the HG weight, Fig. 17. Here, HGs with lattice designs are the lightest and consequently the increase of thermal capacitance is the least pronounced. Also, the HGs' contribution to the overall weight of the stator-winding assembly is relatively low from 3% to 4% (epoxy impregnated stator-winding assembly with no housing is considered here).

C. Three-Phase Ac Effects

As discussed earlier, the motorette analysis is insufficient to provide a complete quantitive information regarding power losses generated in the machine assembly. This is due to absence of the winding neighbouring phases and rotor PM magnetic flux among other reasons. These effects however, would require the complete machine to be properly assessed experimentally. In this analysis a simplified theoretical illustration is used instead.

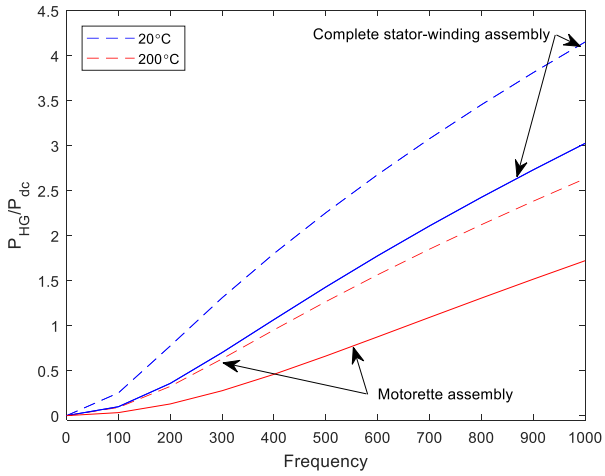

Fig. 18. Frequency variation of HG power loss contribution in reference to the winding dc power loss (P_{HG}/P_{dc}) for motorette with solid body HG

Fig. 18 presents results from 3D FEAs of the HG's power loss contribution for both motorette and complete stator-winding assemblies. Here the motorette with solid HG is considered. As expected, the magnetic flux leakage between neighbouring phases has a detrimental effect on the HG performance. This results in 36% increase of the power loss generated in the HG. Although, the increase might appear to be considerable, it was derived for the worst case scenario, i.e. HGV1 with Al-1350. Thus, the overall power loss for alternative HG designs (HGV2-HGV6) and material (AlSi10Mg) is expected to remain relatively small. Here, the best HG variant generates 5% of additional power loss at 1kHz, Fig. 11. The rotational ac effects associated with PM rotor flux leakage are not considered here, as these are beyond the scope of this feasibility study. However, it is expected that the effects are non-negligible particularly for motor designs employing the open-slot stator topology [8].

V. Observations and Conclusions

This feasibility study has shown that passive HGs can be designed and manufactured to assure enhanced heat transfer from the winding body and insignificant additional power loss to the overall system (complete machine assembly). The initial results suggest approximately 40% increase in input power handling at low-frequency operation and 20% improvement at high-frequency for the analysed case study. The theoretical predictions have been validated experimentally showing good correlation with measurements. It has been shown that material properties of the HG hardware differ from the initially assumed material data. In particular, higher electrical resistivity of aluminium alloys commonly used in SLM, like AlSi10Mg, assures reduced HG power loss. The material thermal conductivity is also affected, but here with insignificant impact on the heat transfer capability [15]. The additive manufacturing employed in fabrication of the alternative HGs enabled light-weight, low-power loss and good thermal conductivity design solutions. The measured thermal performance has shown significant improvement of dissipative heat transfer from the winding body. Here, 55% to 85% increase of the winding-to-stator thermal conductance has been observed. All these highlight the potential of the proposed approach for enhancing heat removal in electrical machines, but also emphasise the

importance of incorporating experimental work in the design process. Clearly, more experimental work is required to fully validate and understand all HG performance measures. In particular, HG thermal behaviour and material physical properties in the broader context of complete machine assembly will be investigated by the authors as a continuation of this proof of concept study.

ACKNOWLEDGMENT

The authors wish to thank Advanced Propulsion Centre (APC) UK for supporting this research.

REFERENCES

[1] D. A. Reay, P. A. Kew, R. McGlen, "Heat Pipes: Theory, Design and Applications," Elsevier, 2013.

[2] T. Hasset, M. Hodowanec, "Electric Motor with Heat Pipes," United States Patent, US 7569955 B2, 2009.

[3] M. Bradford, "The Application of Heat Pipes to Cooling Rotating Electrical Machines," *IET International Conference on Electrical Machines and Drives*, pp. 145 – 149, 1989.

[4] M. Popescu, D. A. Staton, A. Boglietti, A. Cavagnino, D. Hawkons, J. Goss, "Modern Heat Extraction Systems for Power Traction Machines – A Review," *IEEE Transactions on Industry Applications*, vol. 52, no. 3, pp. 2167 – 2175, May/June 2016.

[5] S. Ayat, R. Wrobel, J. Goss, D. Drury, "Experiment Informed Methodology for Thermal Design of PM Machines," *11th International Conference on Ecological Vehicles and Renewable Energies (EVER)*, pp. 1 – 7, April 2016.

[6] J. Godbehere, R. Wrobel, D. Drury, P. H. Mellor, "Experimentally Calibrated Thermal Stator Modelling of AC Machines for Short-Duty Transient Operation," *IEEE Transactions on Industry Applications*, vol. 53, no. 4, pp. 3457 – 3466, July/August 2017.

[7] R. Wrobel, D. E. Salt, A. Griffo, N. Simpson, P. H. Mellor, "Derivation and Scaling of AC Copper Loss in Thermal Modelling of Electrical Machines," *IEEE Transactions on Industrial Electronics*, vol. 61, no. 8, pp. 4412 – 4420, August 2014.

[8] R. Wrobel, N. Simpson, P. H. Mellor, J. Goss, D. A. Staton, "Design od a Brushless PM Starter Generator for Low-Cost Manufacture and High-Aspect-Ratio Mechanical Space Envelope," *IEEE Transactions on Industry Applications*, vol. 53, no. 2, pp. 1038 – 1048, March/April 2017.

[9] R. Wrobel, D. Staton, R. Lock, J. Booker, D. Drury, "Winding Design for Low-Cost Manufacture in Application to Fixed-Speed PM Generator," *IEEE Transactions on Industry Applications*, vol. 51, no. 5, pp. 3773 – 3782, September/October 2015.

[10] R. Wrobel, P. H. Mellor, D. Holliday, "Thermal Modelling of Segmented Stator Winding Design," *IEEE Transactions on Industry Applications*, vol. 47, no. 5, pp. 2023 – 2030, September/October 2011.

[11] W. Sixel, M. Liu, G. Nellis, B. Sarlioglu, "Cooling of Windings in Electrical Machines via 3D Printed Heat Exchanger," *IEEE Energy Conversion Congress and Exposition (ECCE)*, pp. 229 – 235, September 2018.

[12] S. Ayat, C. Serghine, T. Kolonowski, S. Yon, A. Mutabazi, S. McDaniel, "The use of Phase Change Material for the Cooling of Electric Machine Windings formed with Hollow Conductors," *IEEE International Electric Machines and Drives Conference (IEMDC)*, pp. 1195 – 1201, May 2019.

[13] A. Reinap, F. J. Marquez-Fernandez, M. Alakula, R. Deodhar, K. Mishima, "Direct Conductor Cooling in Concentrated Windings," *XXIIIrd International Conference on Electrical Machines (ICEM)*, pp. 2654 – 2660, Sptember 2018.

[14] P. Lindh, I. Petrov, J. Pyrhonen, M. Niemela, P. Immonen, E. Scherman, "Direct Liquid Cooling Method verified with a Permanent-Magnet Motor in a Bus," *IEEE Transactions on Industry Applications*, pp. 1 – 8, (early access article).

[15] R. Wrobel, A. Hussein, "Design Considerations of Heat Guides Fabricated Using Additive Manufacturing for Enhanced Heat Transfer in Electrical Machines," *IEEE Energy Conversion Congress and Exposition (ECCE)*, pp. 6506 – 6513, September 2018.

[16] J. Goss, M. Popescu, D. Staton, R. Wrobel, J. Yon, P. Mellor, "A Comparision between Maxium Torque/Ampere Efficiency Control Strategies in IPM Synchronous Machines," *IEEE Energy Conversion Congress and Exposition (ECCE)*, pp. 2403 – 2410, 2014.

[17] N. Simpson, R. Wrobel, P. H. Mellor, "Estimation of Equivalent Thermal Parameters of Impregnated Electrical Windings," *IEEE Transactions on Industry Applications*, vol. 49, no. 6, pp. 2505 – 2515, November/ December 2013.

[18] J. Fletcher, B. Williams, M. Mahmoud, "Airgap Fringing Fux Reduction in Inductors Using Open-Circuit Copper Screens," *IEE Proceedings – Electric Power Applications*, vol. 152, no. 4, pp. 990 – 996, July 2005.

[19] R. Camilleri, D. A. Howey, M. D. McCulloch,"Experimental Investigation of the Thermal Contact Resistance in Shrink Fit Assemblies with Relevance to Electrical Machines," *IET International Conference on Power Electronics, Machines and Drives (PEMD)*, pp. 1 – 9, 2014.

[20] C. Silbernagel, I. Ashcroft, P. Dickens, M. Galea, "Electrical Resistivity of Additevely Manufactured AlSi10Mg for Use in Electric Motors," *Elsevier, Additive Manufacturing*, vol. 21, pp. 395 – 403, May 2018.

[21] X. Zhao, B. Song, W. Fan, Y. Zhang, Y. Shi, "Selective Laser Melting of Carbon/AlSi10Mg Composities: Microstructure, Mechanical and Electronical Properties," *Elsevire, Journal of Alloys and Compounds*, vol. 665, pp. 271 – 281, April 2016.

[22] Reinshaw Material Data Sheet, "AlSi10Mg-0403 Powder for Additive Manufacturing," 2015

[23] R. P. Wojda, M. K. Kazimierczuk, "Winding Resistance of Litz-Wire and Multi-Strand Inductors," *IET Power Electronics*, vol. 5, pp. 257-268, 2012.

[24] P. Mellor, R. Wrobel, N.Simpson, "Ac Loss in High Frequency Electrical Machine Widimgs Formed from Large Section Conductrors," *IEEE Energy Conversion Congress and Exposition (ECCE)*, pp. 5563 – 5570, September 2014.

[25] R. Wrobel, A. Ayat, J. Godbehere, "A Systematic Experimental Approach in Deriving Stator-Winding Heat Transfer," *IEEE International Electric Machines and Drives Conference (IEMDC)*, pp. 1 – 8, May 2017.

[26] C. Wohlers, P. Juris, S. Kabelac, B. Ponick, "Design and Direct Liquid Cooling of Tooth-Coil Winding," *Electrical Engineering, Springer*, vol. 100, no. 4, pp. 2299 – 2308, December 2018.

[27] P. Lindh, I. Petrov, J. Pyrhonen, E. Scherman, M. Niemela, P. Immonen"Direct Liquid Cooling Method Verified with a Permanent-Magnet Traction Motor in a Bus," *IEEE Transactions on Industry Applications*, vol. 55, no. 4, pp. 4183 – 4191, July/August 2019.

[28] M. C. Kulan, N. J. Baker, "Development of a Thermal Equivalent circuit to Quantify the Effect of Thermal Paste on Heat Flow Through a Permanent Magnet Alternator," IEEE Transactions on Industry Applications, vol. 55, no. 2, pp. 1261 – 1271, March/April 2019.

[29] H. Liu, S. Ayat, R. Wrobel, C. Zhang, "Comparative Study of Thermal Properties of Electrical Windings Impregnated with Alternative Varnish Materials" IET The Journal of Engineering, vol. 2019, no. 17, pp. 2736 – 3741, June 2019.

[30] V. Madonna, A. Walker, P. Giangrande, G. Serra, C. Gerada, M. Galea, "Improved Thermal Management and Analysis for Stator End-Windings of Electrical MAchines," IEEE Transactions on Industrial Electronics, vol. 66, no. 7, pp. 5057-5069, July 2019.